Inorganic Chemistry
Article

Inorg. Chem. **2010**, *49*, 4301–4306 **4301**
DOI: 10.1021/ic100188w

Three-Dimensional Porous Metal−Organic Frameworks Exhibiting Metamagnetic Behaviors: Synthesis, Structure, Adsorption, and Magnetic Properties

Qun Yu, Yong-Fei Zeng, Jiong-Peng Zhao, Qian Yang, Bo-Wen Hu, Ze Chang, and Xian-He Bu*

Department of Chemistry, and TKL of Metal- and Molecule-Based Material Chemistry, Nankai University, Tianjin 300071, P. R. China

Received January 30, 2010

Two isomorphous 3D porous metamagnets, $\{[M_6(N_3)_{12}\mathbf{L}_6]\cdot(H_2O)_{13}\}_\infty$ (M = Ni^{II}, **1**; Co^{II}, **2**), have been constructed from 2-(1,3,4-thiadiazol-2-ylthio)acetic acid (H**L**), with azido as the auxiliary ligand. Single-crystal X-ray analysis indicates that the complexes possess hexagonal channels with dimensions of about 8.3 Å × 8.3 Å along the *c* axis and void space of about 25% per cell volume. Hydrogen adsorption measurements at 740 Torr and 77 K reveal that hydrogen uptakes of 0.68 and 0.83 wt % were observed in **1** and **2**, respectively, with BET surface areas of 309 and 328 m^2/g. Magnetic measurement reveals that both of them exhibit global metamagnetic behaviors resulted from strong intrachain ferromagnetic couplings and weak interchain antiferromagnetic interactions, with critical fields of 22 kOe and 6 kOe for **1** and **2**, respectively.

Introduction

The investigation of porous metal−organic frameworks (PMOFs) or porous coordination polymers (PCPs) has raised intense interest for their promising applications in gas storage,[1] separation,[2] drug delivery,[3] and catalysis.[4] One of the most active topics in this area is the design of new PMOFs or PCPs with other physical/chemical properties, for example, conductivity, chirality,[5] luminescence,[6] and magnetism.[7] As for the system of porous magnets, there had been a prevalent opinion that porosity and long-range magnetic ordering were a paradox and difficult to observe simultaneously in the same system.[8] However, numerous studies in recent years have clarified that both of them are no longer contradictive, but there is a competitive-but-not-incompatible relation.[9] To construct porous magnets, one key point is to fulfill effective magnetic exchange pathways in the porous MOFs.[10] As a relatively rare magnetic phenomenon, metamagnetic behavior may occur if the interactions are weak enough to be overcome by an external field and enter into another magnetic state which is along with the reorientation

*Author to whom correspondence should be addressed. Fax: +86-22-23502458. E-mail: buxh@nankai.edu.cn.

(1) (a) Eddaoudi, M.; Moler, D. B.; Li, H.; Chen, B.; Reineke, T. M.; O′Keeffe, M.; Yaghi, O. M. *Acc. Chem. Res.* **2001**, *34*, 319. (b) Matsuda, R.; Kitaura, R.; Kitagawa, S.; Kubota, Y.; Belosludov, R. V.; Kobayashi, T. C.; Sakamoto, H.; Chiba, T.; Takata, M.; Kawazoe, Y.; Mita, Y. *Nature* **2005**, *436*, 238. (c) Moulton, B.; Zaworotko, M. *J. Chem. Rev.* **2001**, *101*, 1629. (d) Dincă, M.; Yu, A. F.; Long, J. R. *J. Am. Chem. Soc.* **2006**, *128*, 8904. (e) Bu, X.-H.; Tong, M.-L.; Chang, H.-C.; Kitagawa, S.; Batten, S. R. *Angew. Chem., Int. Ed.* **2004**, *43*, 192.

(2) (a) Pan, L.; Olson, D. H.; Ciemnolonski, L. R.; Heddy, R.; Li, J. *Angew. Chem., Int. Ed.* **2006**, *45*, 616. (b) Zhang, Z. M.; Yao, S.; Li, Y. G.; Clérac, R.; Lu, Y.; Su, Z. M.; Wang, E. B. *J. Am. Chem. Soc.* **2009**, *131*, 14600. (c) Li, J. R.; Kuppler, R. J.; Zhou, H. C. *Chem. Soc. Rev.* **2009**, *38*, 1498. (d) Li, J. R.; Tao, Y.; Yu, Q.; Bu, X. H.; Sakamoto, H.; Kitagawa, S. *Chem.—Eur. J.* **2008**, *14*, 2771. (e) He, H.; Cao, G. J.; Zheng, S. T.; Yang, G. Y. *J. Am. Chem. Soc.* **2009**, *131*, 15588.

(3) (a) Horcajada, P.; Serre, C.; Vallet-Regí, M.; Sebban, M.; Taulelle, F.; Férey, G. *Angew. Chem., Int. Ed.* **2006**, *45*, 5974. (b) Horcajada, P.; Serre, C.; Maurin, G.; Ramsahye, N. A.; Balas, F.; Vallet-Regí, M.; Sebban, M.; Taulelle, F.; Férey, G. *J. Am. Chem. Soc.* **2008**, *130*, 6774.

(4) (a) Llabrési Xamena, F. X.; Abad, A.; Corma, A.; García, H. *J. Catal.* **2007**, *250*, 294. (b) Alaerts, L.; Séguin, E.; Poelman, H.; Thibault-Starzyk, F.; Jacobs, P. A.; De Vos, D. E. *Chem.—Eur. J.* **2006**, *12*, 7353. (c) Horcajada, P.; Surblé, S.; Serre, C.; Hong, D. Y.; Seo, Y. K.; Chang, J. S.; Grenèche, J. M.; Margiolaki, I.; Férey, G. *Chem. Commun.* **2007**, 2820.

(5) (a) Inoue, K.; Kikuchi, K.; Ohba, M.; Oh kawa, H. *Angew. Chem., Int. Ed.* **2003**, *42*, 268. (b) Li, C. R.; Li, S. L.; Zhang, X. M. *Cryst. Growth Des.* **2009**, *9*, 1702.

(6) (a) Ohkoshi, S. i.; Toroko, H.; Hozumi, T.; Zhang, Y.; Hashimoto, K.; Mathonière, C.; Bord, I.; Rombaut, G.; Verelst, M.; dit Moulin, C. C.; Villain, F. *J. Am. Chem. Soc.* **2006**, *128*, 270. (b) Wang, M. S.; Guo, S. P.; Li, Y.; Cai, L. Z.; Zou, J. P.; Xu, G.; Zhou, W. W.; Zheng, F. K.; Guo, G. C. *J. Am. Chem. Soc.* **2009**, *131*, 13572. (c) Xu, B.; Lü, J.; Cao, R. *Cryst. Growth Des.* **2009**, *9*, 3003.

(7) (a) Xiang, S.; Wu, X.; Zhang, J.; Fu, R.; Hu, S.; Zhang, X. *J. Am. Chem. Soc.* **2005**, *127*, 16352. (b) Fang, Z. L.; Yu, R. M.; He, J. G.; Zhang, Q. S.; Zhao, Z. G.; Lu, C. Z. *Inorg. Chem.* **2009**, *48*, 7691. (c) Zeng, Y. F.; Hu, X.; Liu, F. C.; Bu, X. H. *Chem. Soc. Rev.* **2009**, *38*, 469. (d) Zhao, W.; Song, Y.; Okamura, T.; Fan, J.; Sun, W. Y.; Ueyama, N. *Inorg. Chem.* **2005**, *44*, 3330. (e) Liu, C. M.; Zhang, D. Q.; Zhu, D. B. *Inorg. Chem.* **2009**, *48*, 792. (f) Gu, Z. G.; Song, Y.; Zuo, J. L.; You, X. Z. *Inorg. Chem.* **2007**, *46*, 9522. (g) Rombaut, G.; Verelst, M.; Golhen, S.; Ouahab, L.; Mathonière, C.; Kahn, O. *Inorg. Chem.* **2001**, *40*, 1151. (h) Neville, S. M.; Halder, G. J.; Chapman, K. W.; Duriska, M. B.; Southon, P. D.; Cashion, J. D.; Létard, J. F.; Moubaraki, B.; Murray, K. S.; Kepert, C. J. *J. Am. Chem. Soc.* **2008**, *130*, 2869. (i) Jürgens, O.; Vidal-Gancedo, J.; Rovira, C.; Wurst, K.; Sporer, C.; Bildstein, B.; Schottenberger, H.; Jaitner, P.; Veciana, J. *Inorg. Chem.* **1998**, *37*, 4547.

(8) (a) Wang, Z. M.; Zhang, B.; Fujiwara, H.; Kobayashi, H.; Kurmoo, M. *Chem. Commun.* **2004**, 416. (b) Férey, G. *Nat. Mater.* **2002**, *1*, 91. (c) Maspoch, D.; Ruiz-Molina, D.; Veciana, J. *J. Mater. Chem.* **2004**, *14*, 2713.

Published on Web 04/05/2010

of spin.[11] Frequently, such interactions are not strong and are exhibited in intermolecule, interchain, and interlayer interactions mediated by long linkers, blocking groups, hydrogen bonds, and $\pi-\pi$ interactions.[12]

In this contribution, we choose a new ligand, 2-carboxymethylmercapto-1,3,4-thiadiazole acid (**HL**), which contains both carboxylate and thiadiazole groups,[13] as a bridging ligand to synthesize a porous metamagnet, due to the following considerations: (1) a ligand with two different functional groups that are well separated may facilitate a 3D porous MOF; (2) the long acetic groups containing σ bonds would not conduct strong magnetic couplings that may be overcome by an external field, which would exhibit metamagntic behavior; (3) azido,[14] a well-known bridging ligand, was introduced to this system and can readily form EO (end-on) N_3^-/μ_2-N,N′-diazole and EO-N_3^-/*syn-syn*-COO^- units because the M···M distances bridged by EO azido,[15] *syn-syn*-COO^-, and μ_2-N,N′-diazole are very similar, which may result in ferromagnetic couplings due to orbital countercomplementarity in EO-N_3^-/μ_2-N,N′-diazole and EO-N_3^-/*syn-syn*-COO^- units.[16]

Herein, we report two isomorphic azide-bridged 3D frameworks $\{[M_6(N_3)_{12}\mathbf{L}_6]\cdot(H_2O)_{13}\}_\infty$ (M = Ni^{II}, **1**; Co^{II}, **2**), in which alternating EO-N_3^-/μ_2-N,N′-diazole and EO-N_3^-/*syn-syn*-COO^- groups bridge metal ions to form a 1D chain which is further extended to 3D porous frameworks through the L^- ligand. In **1** and **2**, 1D hexagonal channels were observed, which are occupied by 1D H-bond water chains. Gas adsorption measurements of **1** and **2** confirm their permanent porosity, possessing hexagonal channels with pore sizes of about 8.3 Å for **1** and 8.7 for **2** along the *c* axis and a void space of about 25%. Magnetic susceptibility measurements exhibit that **1** and **2** show metamagnetic behaviors with a critical field of 22 KOe and 6 kOe, respectively, which can be accounted for by 1D ferromagnetic chains with two types of orbital countercomplemetary magnetic pathways of EO-N_3^-/μ_2-N,N′-diazole and EO-N_3^-/*syn-syn*-COO^- and interchian antiferromagnetic coupling.

Experimental Section

Materials and General Methods. All solvents and starting materials for synthesis were purchased commercially and were used as received. 2-Carboxymethylmercapto-1,3,4-thiadiazole acid (**HL**) was synthesized according to literature methods.[13a] IR spectra were measured on a Tensor 27 OPUS (Bruker) FT-IR spectrometer with KBr pellets. Elemental analyses (C, H, N) were performed on a Perkin-Elmer 240C analyzer. The X-ray powder diffraction (XRPD) was measured on a Rigaku D/Max-2500 diffractometer at 40 kV and 100 mA with a Cu-target tube and a graphite monochromator. Simulations of the XRPD spectra were carried out by the single-crystal data and diffraction-crystal module of the Mercury (Hg) program, available free of charge via the Internet at http://www.iucr.org. The thermogravimetric analysis (TGA) was done on a standard TG-DTA analyzer under an air atmosphere at a heating rate of 10 °C/min for measurement. Magnetic data were collected using crushed crystals of the sample on a Quantum Design MPMS-XL SQUID magnetometer. The data were corrected using Pascal's constants to calculate the diamagnetic susceptibility. Adsorption/desorption experiments were carried out at the temperature of liquid nitrogen (77 K). To remove the H_2O molecules residing in the open channels, the complexes were first soaked in MeOH and then heated in a sample tube under a vacuum at a temperature of 100 °C until the pressure in the manifold reached 3 μmHg and was kept at that pressure and temperature for at least 5 h. Samples were transferred between manifolds in sample tubes sealed with transeals. Hydrogen and nitrogen adsorption/desorption isotherms were measured using a Micromeritics ASAP 2020 M and 99.999% pure N_2 and H_2.

Syntheses of Complexes 1 and 2. **$[Ni_6(N_3)_6\mathbf{L}_6]\cdot(H_2O)_{13}$ (1).** A buffer layer of a mixture of methanol and distilled water (V/V = 1:1, 12 mL) was carefully layered over a distilled water (2 mL) solution of the mixture of **HL** ligand (0.1 mmol) and NaN_3 (0.3 mmol). Then, a solution of $Ni(NO_3)_2\cdot6H_2O$ (0.3 mmol) in methanol (2 mL) was layered over the buffer layer. This was left undisturbed at room temperature, and then pure prism green crystals were harvested after about four weeks. Yield: ~20% (based on **HL**). Anal. Calcd for $C_{24}H_{44}N_{30}Ni_6O_{25}S_{12}$: C, 15.25; H, 2.35; N, 22.23%. Found: C, 15.64; H, 2.90; N, 22.09%. IR (KBr, cm^{-1}): 3418 m, 2090vs, 1628vs, 1521w, 1402vs, 1304w, 1218w, 1109s, 1031 m, 895w, 724 m, 665w.

$[Co_6(N_3)_6\mathbf{L}_6]\cdot(H_2O)_{13}$ (2). A procedure similar to that for **1** was followed except that $Ni(NO_3)_2\cdot6H_2O$ was replaced by $Co(CH_3COO)_2\cdot6H_2O$. Yield: ~30% (based on **HL**). Anal. Calcd. for $C_{24}H_{44}N_{30}Co_6O_{25}S_{12}$: C, 15.24; H, 2.34; N, 22.22%. Found: C, 15.44; H, 2.78; N, 22.73%. IR (KBr, cm^{-1}): 3415 m, 2090vs, 1622vs, 1521w, 1407vs, 1291 m, 1245 m, 1107s, 1029 m, 897w, 720 m, 663w.

Caution! *Azido complexes are potentially explosive in the presence of organic compounds. Only a small amount of material should be prepared and should handled with care.*

X-Ray Crystallographic Studies. X-ray single-crystal diffraction data for complexes **1** and **2** were collected on a Rigaku RAXIS-RAPID diffractometer with Mo Kα radiation (λ = 0.71073 Å). The program SAINT[17] was used for integration of the diffraction profiles. All of the structures were solved by direct methods using the SHELXS program of the SHELXTL

(9) (a) Huang, Y. G.; Yuan, D. Q.; Pan, L.; Jiang, F. L.; Wu, M. Y.; Zhang, X. D.; Wei, W.; Gao, Q.; Lee, J. Y.; Li, J.; Hong, M. C. *Inorg. Chem.* **2007**, *46*, 9609. (b) Wang, Z. M.; Zhang, B.; Kurmoo, M.; Green, M. A.; Fujiwara, H.; Otsuka, T.; Kobayashi, H. *Inorg. Chem.* **2005**, *44*, 1230. (c) Xiang, S.; Wu, X.; Zhang, J.; Fu, R.; Hu, S.; Zhang, X. *J. Am. Chem. Soc.* **2005**, *127*, 16352. (d) Pinkowicz, D.; Podgajny, R.; Bałanda, M.; Makarewicz, M.; Gaweł, B.; Łasocha, W.; Sieklucka, B. *Inorg. Chem.* **2008**, *47*, 9745.

(10) (a) Beobide, G.; Wang, W.; Castillo, O.; Luque, A.; Román, P.; Tagliabue, G.; Galli, S.; Navarro, J. A. R. *Inorg. Chem.* **2008**, *47*, 5267. (b) Fang, Z. L.; Yu, R. M.; He, J. G.; Zhang, Q. S.; Zhao, Z. G.; Lu, C. Z. *Inorg. Chem.* **2009**, *48*, 7691.

(11) (a) Das, A.; Rosair, G. M.; Salah El Fallah, M.; Ribas, J.; Mitra, S. *Inorg. Chem.* **2006**, *45*, 3301. (b) Hao, X.; Wei, Y.; Zhang, S. *Chem. Commun.* **2000**, 2271. (c) Viau, G.; Lombardi, M. G.; Munno, G. D.; Julve, M.; Lloret, F.; Faus, J.; Caneschic, A.; Clemente-Juan, J. M. *Chem. Commun.* **1997**, 1195.

(12) (a) Mukherjee, P. S.; Dalai, S.; Zangrando, E.; Lloretc, F.; Chaudhuri, N. R. *Chem. Commun.* **2001**, 1444. (b) Liu, T.; Zhang, Y.; Wang, Z.; Gao, S. *Inorg. Chem.* **2006**, *45*, 2782. (c) Ribas, J.; Monfort, M.; Diaz, C.; Bastos, C.; Solan, X. *Inorg. Chem.* **1994**, *33*, 484.

(13) (a) Xue, D. X.; Zhang, W. X.; Chen, X. M. *J. Mol. Struct.* **2008**, *877*, 36. (b) Wang, Y.; Zhang, L.; Fan, Y.; Hou, H.; Shen, X. *Inorg. Chim. Acta* **2007**, *360*, 2958. (d) Wang, Y.; Yin, M.; Fan, Y.; Hou, H. *J. Coord. Chem.* **2008**, *61*, 907. (e) Xue, D. X.; Zhang, W. X.; Chen, X. M.; Wang, H. Z. *Chem. Commun.* **2008**, 1551.

(14) (a) Ma, Y.; Zhang, J. Y.; Cheng, A. L.; Sun, Q.; Gao, E. Q.; Liu, C. M. *Inorg. Chem.* **2009**, *48*, 6142. (b) Milios, C. J.; Prescimone, A.; Sanchez-Benitez, J.; Parsons, S.; Murrie, M.; Brechin, E. K. *Inorg. Chem.* **2006**, *45*, 7053. (c) Rajendiran, T. M.; Mathonière, C.; Golhen, S.; Ouahab, L.; Kahn, O. *Inorg. Chem.* **1998**, *37*, 2651.

(15) (a) Georgopoulou, A. N.; Raptopoulou, C. P.; Psycharis, V.; Ballesteros, R.; Abarca, B.; Boudalis, A. K. *Inorg. Chem.* **2009**, *48*, 3167. (b) Cheng, X. N.; Zhang, W. X.; Chen, X. M. *J. Am. Chem. Soc.* **2007**, *129*, 15738. (c) Zeng, Y. F.; Liu, F. C.; Zhao, J. P.; Cai, S.; Bu, X. H.; Ribas, J. *Chem. Commun.* **2006**, 2227. (d) Ribas, J.; Escuer, A.; Monfort, M.; Vicente, R.; Cortés, R.; Lezama, L.; Rojo, T. *Coord. Chem. Rev.* **1999**, *193*, 1027. (e) Hu, B. W.; Zhao, J. P.; Sañudo, E. C.; Liu, F. C.; Zeng, Y. F.; Bu, X. H. *Dalton Trans.* **2008**, 5556. (f) Lin, H. M.; Chang, T. Y. *Cryst. Growth Des.* **2009**, *9*, 2988.

(16) Khan, O. *Molecular Magnetism*; VCH: New York, 1993.

(17) *SAINT Software Reference Manual*; Bruker AXS: Madison, WI, 1998.

Table 1. Crystallographic Data and Structure Refinement Summary for Complexes **1** and **2**

	1	**2**
chemical formula	$C_{24}H_{44}N_{30}Ni_6O_{25}S_{12}$	$C_{24}H_{44}N_{30}Co_6O_{25}S_{12}$
fw	1889.73	1891.17
space group	$R\bar{3}c$	$R\bar{3}c$
a/Å	24.342(3)	24.502(4)
b/Å	24.342(3)	24.502(4)
c/Å	18.303(4)	18.450(4)
V/Å^3	9392(3)	9592(3)
D/g cm^{-3}	1.977	1.937
Z	6	6
μ/mm^{-1}	2.267	2.010
$R1$ [$I > 2\sigma(I)$]	0.0418	0.0480
$wR2$ (all data)	0.0974	0.1680
goodness-of-fit on F^2	1.158	1.162
$(\Delta\rho)$max, $(\Delta\rho)$min/e Å^{-3}	1.344, −1.103	1.873, −1.172

package and refined by full-matrix least-squares methods with SHELXL.[18] Metal atoms in each complex were located from the *E*-maps, and other non-hydrogen atoms were located in successive difference Fourier syntheses and refined with anisotropic thermal parameters on F^2. The N5, N7, and N8 of azido are disorderd in both **1** and **2**. Crystallographic data and experimental details for structural analyses are summarized in Table 1. Selected bond lengths and angles are listed in Table S1 (see the Supporting Information). Full crystallographic data for **1** and **2** have been deposited with the CCDC (752985 and 752986). These data can be obtained free of charge from The Cambridge Crystallographic Data Centre via www.ccdc.cam.ac.uk/data_request/cif.

Results and Discussion

Description of the Structure. Single-crystal X-ray diffraction analyses reveal that complexes **1** and **2** are isostructural, so only the structure of **1** is discussed in detail here. Complex **1** crystallizes in the rhombohedral space group of $R\bar{3}c$ (see Table 1). The asymmetric unit of **1** contains one Ni^{II} ion, one $\mathbf{L}^-$ ligand, and two halves of azido anions. As shown in Figure 1a, Ni1 is hexa-coordinated by four nitrogen atoms from two individual $\mathbf{L}^-$ (Ni1−N1 = 2.119 and Ni1−N2B = 2.128 Å) and two individual μ_2-1,1 N_3^- anions (Ni1−N6B = 2.098 and Ni1−N3A = 2.060 Å) and two oxygen atoms from another two individual $\mathbf{L}^-$ groups (Ni1−O2D = 2.043 and Ni1−O1C = 2.040 Å) to complete a distorted octahedral geometry. Both the Ni−N and Ni−O bond distances fall into the range of normal values of nickel complexes.[19] The deprotonated $\mathbf{L}^-$ acts as a tetradentate bridging mode to connect four Ni^{II} ions which consist of *syn-syn* carboxylate and μ_2-N,N′ thiadiazole (Figure S1, Supporting Information), while the azide anions bridge the Ni^{II} ion in EO mode with the Ni−N−Ni angles of 108.22(2) and 116.97(3)°. The EO azido together with thiadiazole and carboxylate groups connect Ni^{II} ions to form an alternating N_3^-/thiadiazole and N_3^-/COO^- chain, with the adjacent Ni···Ni distances of 3.400(4) and 3.514(8) Å (Figure 1b). This is a new azido chain with mixed bridges, which is evidently different from the reported chains which contain one or two bridge groups.[20] The chain is further connected with three neighboring chains through the bridging $\mathbf{L}^-$ groups to form a 3D network, with hexagonal channels along the *c* axis (Figure 1c). Interestingly, water molecules filling in these hexagonal channels are further extended to 1D water chain *via* hydrogen bond interactions. These 1D water chains interact with the 3D framework through strong hydrogen bonds. The solvent-accessible volume estimated by using *PLATON* software is about 25% per cell volume.[21] It is worth noting that all the $-CH_2-$ arms

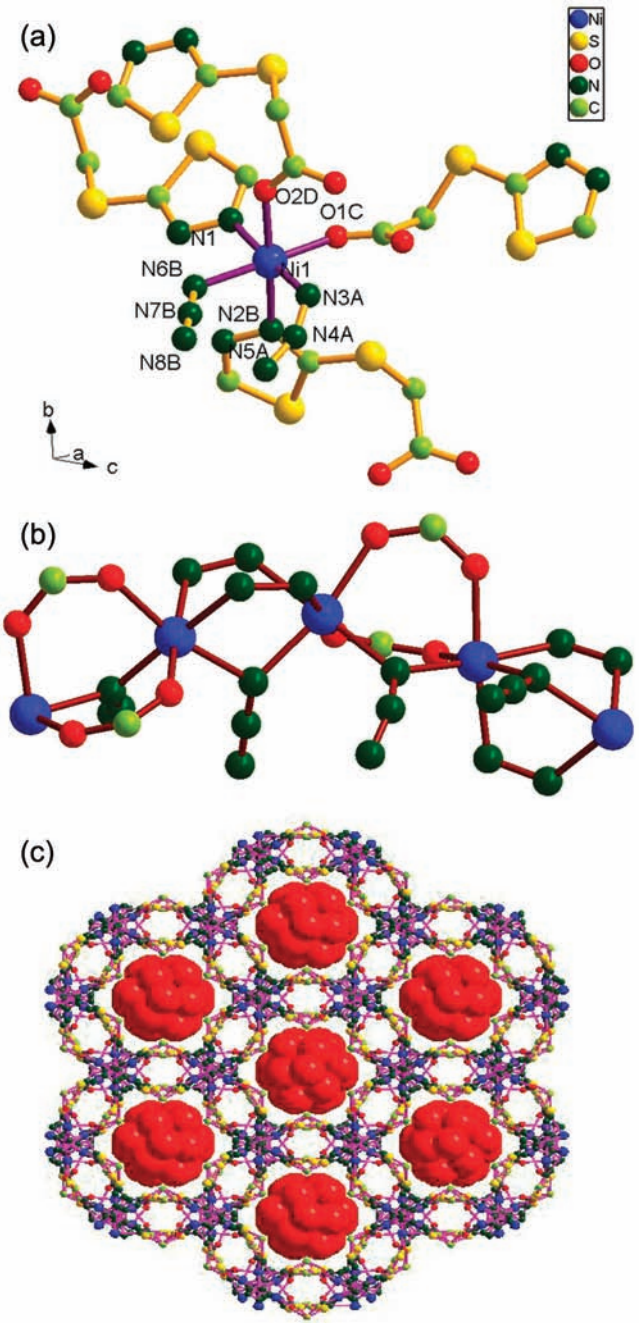

Figure 1. (a) Coordination environment of the Ni^{II} ion in complex **1**. (b) 1D EO-N_3^-/μ_2-N,N′-thiadiazole and EO-N_3^-/*syn-syn*-COO^- in **1**. (c) Porous framework for **1** with hexagonal channels occupied by a 1D water chain. H atoms omitted for clarity.

(18) Sheldrick, G. M. *SHELXTL NT*, version 5.1; University of Gottingen: Gottingen, Germany, 1997.

(19) Schlager, O.; Wieghardt, K.; Nuber, B. *Inorg. Chem.* **1995**, *34*, 6449.

(20) (a) Liu, T. F.; Fu, D.; Gao, S.; Zhang, Y. Z.; Sun, H. L.; Su, G.; Liu, Y. J. *J. Am. Chem. Soc.* **2003**, *125*, 13976. (b) Liu, T.; Zhang, Y. J.; Wang, Z. M.; Gao, S. *Inorg. Chem.* **2006**, *45*, 2782. (c) Ma, Y.; Zhang, J. Y.; Cheng, A. L.; Sun, Q.; Gao, E. Q.; Liu, C. M. *Inorg. Chem.* **2009**, *48*, 6142. (d) Li, J. R.; Yu, Q.; Sañudo, E. C.; Tao, Y.; Bu, X. H. *Chem. Commun.* **2007**, 2602. (e) Zeng, Y. F.; Zhao, J. P.; Hu, B. W.; Hu, X.; Liu, F. C.; Ribas, J.; Ribas-Ariño, J.; Bu, X. H. *Chem.—Eur. J.* **2007**, *13*, 9924.

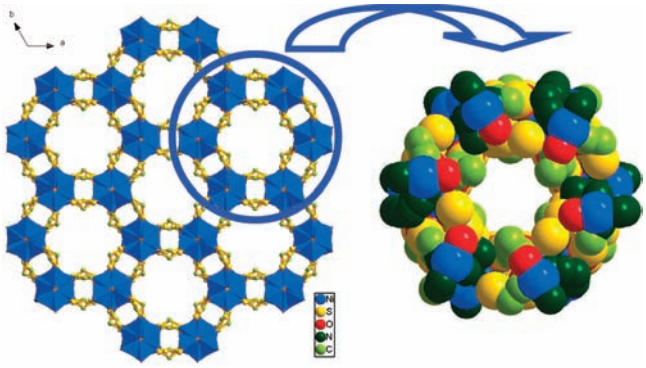

Figure 2. Left: 3D porous network for **1**. Right: Packing diagram for **1** with a pore size of about 8.0 Å.

of the ligand L^- point to the cavity interiors of the hexagonal channel, to result in an L^--decorated inner surface (Figure 2).

TGA and XRPD Analyses. To verify whether the frameworks of complexes **1** and **2** are intact after the removal of free water molecules in hexagonal channels, TGA and X-ray powder diffraction (XRPD) were used to investigate the framework stability and phase purity, respectively. The TGA result of **1** reveals that the lattice water molecules in the hexagonal channels can be easily removed under 100 °C, and the framework of **1** is stable around 320 °C (Figure S2, Supporting Information). The agreement of the powder XRD patterns of the as-synthesized bulk crystals and that simulated from the single-crystal structures of **1** and **2** indicate that the single crystal structures represent the phase purity of samples (Figure S3, Supporting Information). Sample **1a** was obtained by soaking **1** in methanol and then vacuum drying at 100 °C for about 5 h. The similarity of the XRPD patterns of samples as-synthesized and the activated **1a** suggests that the samples are still stable after guest exchange and loss. Sample **2a** was activated as **1a**.

Gas Adsorption Properties. N_2 sorption measurements for activated **1a** and **2a** measured at 77 K revealed a type I isotherm (Figure 3a), which is characteristic of a microporous material.[22] The uptake amount of N_2 increases abruptly at the start of the experiment and reaches a plateau of about 92.6 cm^3 (STP)/g for **1a** and 98.1 cm^3 (STP)/g for **2a**, which correspond to apparent BET surface areas of 309 m^2/g for **1a** and 328 m^2/g for **2a**, respectively. The nitrogen adsorption and desorption are reversible. The median pore sizes are about 0.83 nm for **1a** and 0.87 nm for **2a** (Figure S4, Supporting Information), respectively.

Considering the structure characteristics of **1** and **2** with L^--decorated hexagonal channels, the hydrogen sorption isotherm recorded at 77 K under normal pressure also shows type I behavior. It was found that **1a** can store up to 0.68 wt % (76.4 cm^3/g at standard temperature and pressure (STP)) H_2 at 760 mmHg and 77 K (Figure 3b). This value is comparable to those for porous MOFs with

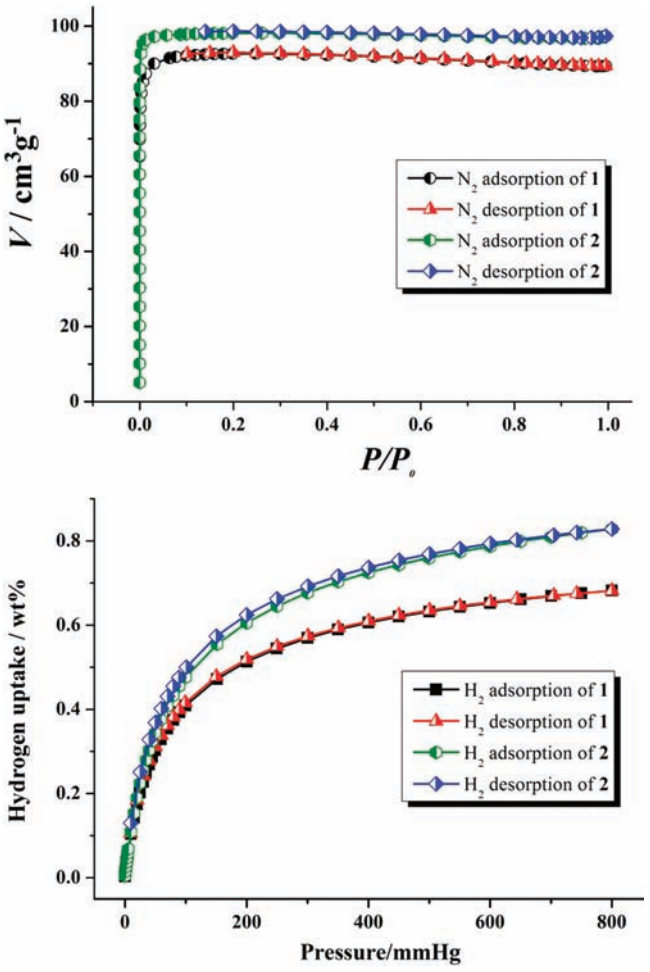

Figure 3. (a) Nitrogen sorption isotherm for **1a** and **2a** at 77 K. (b) Hydrogen sorption isotherm for **1a** and **2a** at 77 K.

larger surface areas; e.g., $[Co_2(6\text{-mna})_2]\cdot 3H_2O$ displays a H_2 uptake of 0.66 wt % with a surface area of 420 m^2/g (CUK-2, CUK = Cambridge University−KRICT, 6-mna = 6-mercapto-3-pyridinecarboxylate (6-mercaptonicotinate)).[23] Hydrogen adsorption measurements show that **2a** can store up to 0.83 wt % (Figure 3b). As shown in Figure 3, the adsorption isotherms for **1a** and **2a** are different, and adsorption/desorption kinetics were very slow in **2a** while quick in **1a**, which may be attributed to the effect of different metal ions in the 3D frameworks.[22b]

Magnetic Properties. Magnetic measurements were carried out on crystalline samples of complexes **1** and **2**. The temperature dependence of $\chi_m T$ for complex **1** as a $\chi_m T$ vs T plot (χ_m is the molar magnetic susceptibility for one Ni^{II}) in the range of 2−300 K, under an applied field of 1 kOe, is shown in Figure 5. The value of $\chi_m T$ at 300 K is 1.37 cm^3 mol^{-1} K, which is of the order expected for one Ni^{II} ion ($g > 2.0$). The $\chi_m T$ values increase smoothly from room temperature until 50 K and then sharply reach a maximum value of 3.61 cm^3 mol^{-1} K at 15 K upon cooling, which was due to the ferromagnetic coupling between the Ni^{II} ions within the chain. Below 15 K, the $\chi_m T$ values dropped to 0.40 cm^3 mol^{-1} K at 2 K, which is

(21) Spek, A. L. *PLATON*; Utrecht University: Utrecht, The Netherlands, 2008.

(22) (a) Rouquerol, F.; Rouquerol, J.; Sing, K. *Adsorption by Powers and Porous Solids*; Academic Press: London, 1999. (b) Kondo, A.; Chinen, A.; Kajiro, H.; Nakagawa, T.; Kato, K.; Takata, M.; Hattori, Y.; Okino, F.; Ohba, T.; Kaneko, K.; Kanoh, H. *Chem.—Eur. J.* **2009**, *15*, 7549.

(23) Humphrey, S. M.; Chang, J. S.; Jhung, S. H.; Yoon, J. W.; Wood, P. T. *Angew. Chem., Int. Ed.* **2007**, *46*, 272.

attributed to zero-field splitting (ZFS) of Ni^{II} ions and antiferromagnetic coupling between the chains.

In spite of the 3D structure of **1**, the main contributions of the magnetic exchange are the EO-N_3^-/μ_2-N,N′-thiadiazole and EO-N_3^-/*syn-syn*-COO^- along the chain, with a weaker contribution of the interchain linkage. By treating the model of alternating F−F chains with $S = 1$, two coupling parameters (J_1 and J_2) were introduced to fit the $\chi_m T$ vs T plot, also taking the interchain interactions (zJ') into account. The Hamiltoninan for the Heisenberg[24] ferromagnetic chain was written as $H = -\sum_{i=1}^{N-1}(J_1 S_{2i}S_{2i+1} + J_2 S_{2i}S_{2i+1})$. The best fit to the model was obtained in the range of 10−300 K with $\alpha < 0.4$ ($\alpha = J_2/J_1$). The best-fit parameters obtained were $J_1 = 131.23\ cm^{-1}$, $J_2 = 48.56\ cm^{-1}$, $\alpha = 0.37$, $g = 2.06$, $zJ' = -1.11\ cm^{-1}$, and $R = 1.57 \times 10^{-5} = \sum(\chi_M^{cal} - \chi_M^{obs})^2/\sum(\chi_M^{obs})^2$.

In **1**, there are two main magnetic pathways (EO-N_3^-/μ_2-N,N′-thiadiazole and EO-N_3^-/*syn-syn*-COO^-) with three types of bridges (*syn-syn* COO^-, EO azido and μ_2-N,N′-thiadiazole). Usually, carboxylate bridges in *syn-syn* configuration provide small metal−metal distances and lead to a good overlap of the magnetic orbitals, which finally promotes antiferromagnetic couplings.[25] The EO azide always conducts ferromagnetic coupling for Ni^{II} systems.[26] The diazole group usually promotes weak antiferromagnetic interactions, with several exceptions of ferromagnetic couplings,[27] which is greatly dependent on the nature of the diazine N−N bridge (e.g., the torsion angle of M−N−N−M and the angle of M−N−N). The coexistence of the EO azide and the *syn-syn* carboxylato bridging ligand leads to a ferromagnetic interaction between the Ni^{II} ions in the chains, which is observed in several reported examples.[26d] However, the combination of EO azido and μ_2-N,N′-diazole mediates ferromagnetic couplings here, which is different from the case in ref 20d in which EO azido groups with large Cu−N_3(EO)−Cu angles transfer antiferromagnetic exchanges. This provides a new example with two types of orbital counter-complementary magnetic pathways: the presence of the antiferromagnetic pathway tends to split into two degenerate antibonding orbitals created by the azido groups, diminishing, thus, the ferromagnetic character, which is consistent with the positive coupling constants. The negative zJ' is associated with the combination of the antiferromagnetic interactions transferred by the L^- ligands and zero-field splitting of Ni^{II} ions.

The field-dependent reduced magnetization per one Ni^{II} ion of **1** at 2 K tends to a statured value of 2.0 $N\beta$ at 5 T and shows a pronounced sigmoid shape at low field. The latter implies metamagnetic behavior for **1** that a magnetic transition occurs from the antiferromagnetic interaction at low field to a ferromagnetic state at high field (Figure 4a), and the critical field defined as dM/dH at 2 K is 22 kOe. To investigate the nature of the metamagnetism of **1**, the low temperature magnetic susceptibilities at different fields were measured. The $\chi_m T$ plot (Figure 4b) shows a cusp around 10.5 K when the applied fields are lower than 20 kOe. The cusp disappears at higher fields, and a plateau occurs at 20 kOe. The negative antiferromagnetic couplings transferred by long L^- groups could be overcome at external fields larger than 22 kOe, and **1** entered into a ferromagnetic state.

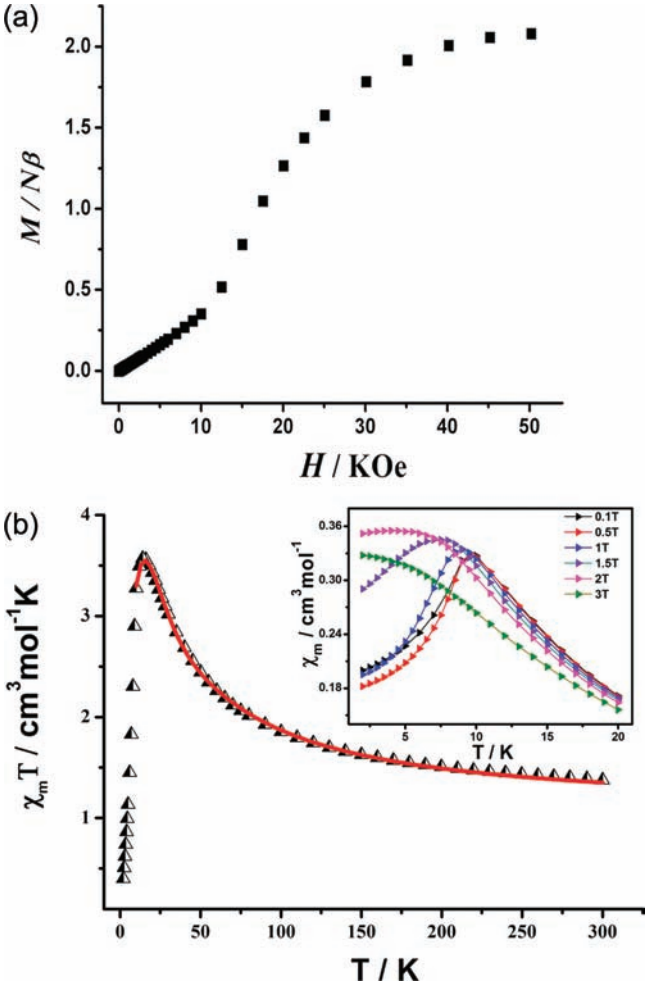

Figure 4. (a) M vs H for **1** measured at 2 K. (b) Temperature dependence of $\chi_m T$ for **1** measured at 1 kOe. The solid line corresponds to the best fit. Inset: the χ_m versus T curves below 20 K at different applied fields for **1**.

The magnetic properties of complex **2** as a $\chi_m T$ vs T plot (χ_m is the molar magnetic susceptibility for one Co^{II}) is shown in Figure 5. The value of $\chi_m T$ at 300 K is 3.43 $cm^3\ mol^{-1}\ K$, which is consistent with that of the Co^{II} ion with a strong spin−orbit coupling. The $\chi_m T$ rises gradually to a local maximum of 3.54 $cm^3\ mol^{-1}\ K$ at 140 K, before dropping to 3.48 $cm^3\ mol^{-1}\ K$ at 60 K. Below 60 K, the $\chi_m T$ values increase more rapidly, reaching a maximum of 4.65 $cm^3\ mol^{-1}\ K$ at 8 K, and finally dropping sharply to 0.29 $cm^3\ mol^{-1}\ K$ at 2 K. The characteristic strong decrease in $\chi_m T$ often seen in Co^{II} complexes as the

(24) Monfort, M.; Resino, I.; Salah El Fallah, M.; Ribas, J.; Solans, X.; Font-Bardia, M.; Stoeckli-Evans, H. *Chem.—Eur. J.* **2001**, *7*, 280.
(25) (a) Rodríguez-Fortea, A.; Alemany, P.; Alvarez, S.; Ruiz, E. *Chem.—Eur. J.* **2001**, *7*, 627. (b) Maji, T. K.; Sain, S.; Mostafa, G.; Lu, T. H.; Ribas, J.; Monfort, M.; Chaudhuri, N. R. *Inorg. Chem.* **2003**, *42*, 709.
(26) (a) Leibeling, G.; Demeshko, S.; Bauer-Siebenlist, B.; Meyer, F.; Pritzkow, H. *Eur. J. Inorg. Chem.* **2004**, 2413. (b) Mialane, P.; Dolbecq, A.; Rivière, E.; Marrot, J.; Sécheresse, F. *Angew. Chem., Int. Ed.* **2004**, *43*, 2274. (c) Aebersold, M. A.; Gillon, B.; Plantevin, O.; Pardi, L.; Kahn, O.; Bergerat, P.; von Seggern, I.; Tuczek, F.; Öhrström, L.; Grand, A.; Lelièvre-Berna, E. *J. Am. Chem. Soc.* **1998**, *120*, 5238. (d) He, Z.; Wang, Z. M.; Gao, S.; Yan, C. H. *Inorg. Chem.* **2006**, *45*, 6694.
(27) (a) Hausmann, J.; Klingele, M. H.; Lozan, V.; Steinfeld, G.; Siebert, D.; Journaux, Y.; Girerd, J. J.; Kersting, B. *Chem.—Eur. J.* **2004**, *10*, 1716. (b) Lozan, V.; Solntsev, P. Y.; Leibeling, G.; Domasevitch, K. V.; Kersting, B. *Eur. J. Inorg. Chem.* **2007**, 3217.

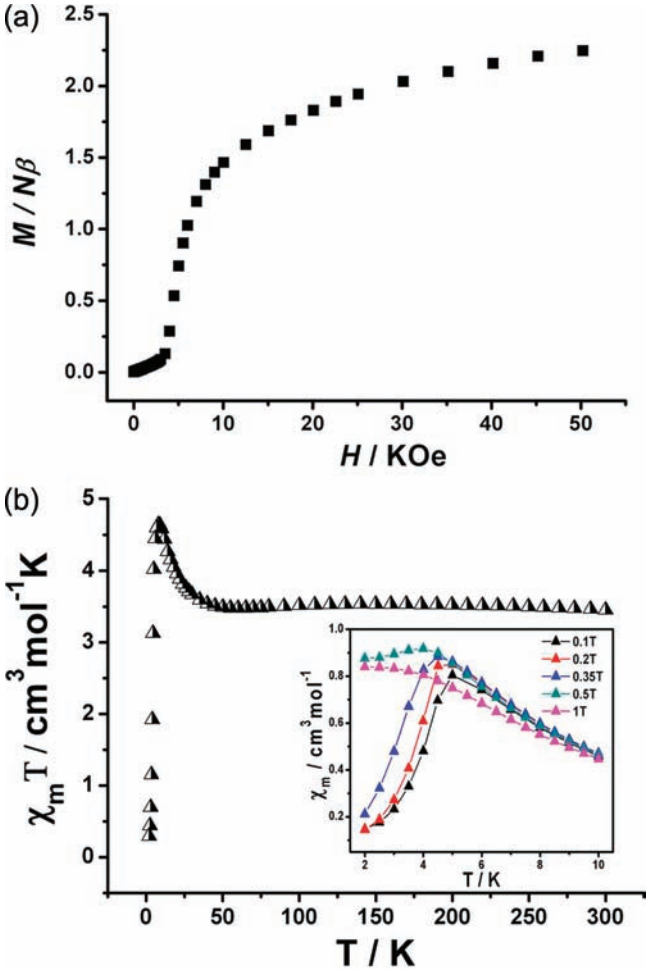

Figure 5. (a) M vs H for **2** measured at 2 K. (b) Temperature dependence of $\chi_m T$ for **2** measured at 1 kOe. Inset: The χ_m versus T curves below 20 K at different applied fields for **2**.

temperature is lowered, due to a strong orbital contribution, is not seen in **1**,[28] which can be interpreted through the combinational results of the partially quenched orbital contribution as cooling for Co^{II} centers and the ferromagnetic exchange interactions between the Co^{II} centers. Similar magnetic behavior has been observed for Co^{II} complexes.[29] The dropping of the $\chi_m T$ plots below 8 K was ascribed to the zero field splitting of Co^{II} ions and antiferromagnetic coupling between the chains.

The field-dependent reduced molar magnetization per one Co^{II} ion in **2** was measured at 2 K and shows a pronounced sigmoid shape at low field that is similar to that of complex **1**. The latter implies metamagnetic behavior for **2** and that a magnetic transition occurs from the antiferromagnetic state at low field to a ferromagnetic state at a high one (Figure 5a), and the critical field defined as dM/dH at 2 K is 6 KOe. To investigate the nature of the metamagnetism of **2**, the low temperature magnetic susceptibility at different fields were measured. The $\chi_m T$ plot (Figure 5b) shows a cusp around 5 K when the applied fields are lower than 5 kOe, and the cusp disappears at higher field. These results indicate that the negative antiferromagnetic couplings transferred by long L^- groups could be overcome at external fields larger than 6 KOe, and **2** entered into a ferromagnetic state.

Conclusion

Two new 3D porous coordination polymers with 1D hexagonal channels decorated by the arms of the ligand have been constructed from the ligand composed of 2-(1,3,4-thiadiazol-2-ylthio)acetic acid and azido, which exhibit magnetic transition from the antiferromagnetic state at low field to a ferromagnetic state at high field, which represents a 3D porous metamagnetic metal−organic frameworks. The introduction of azide as a coligand, which exhibits different magnetic behavior with different coordination modes and angles, represents a feasible approach to achieve the coexistence of porosity and interesting magnetic properties.

Supporting Information Available: X-ray crystallographic files in CIF format for **1** and **2**, tables of bond lengths and angles for **1** and **2**, XRPD patterns for **1** and **2**, and Horvath−Kawazoe differential pore volume plot. This information is available free of charge via the Internet at http://pubs.acs.org.

Acknowledgment. This work was supported by the 973 Program of China (2007CB815305), the NNSF of China (No. 20773068), and the Ph.D. Programs Foundation of MOE of China (200800550001).

(28) (a) Aromí, G.; Stoeckli-Evans, H.; Teat, S. J.; Cano, J.; Ribas, J. *J. Mater. Chem.* **2006**, *16*, 2635. (b) Figgis, B. N.; Gerloch, M.; Lewis, J.; Mabbs, F. E.; Webb, G. A. *J. Chem. Soc. A* **1968**, 2086.

(29) (a) Brechin, E. K.; Cador, O.; Caneschi, A.; Cadiou, C.; Harris, S. G.; Parsons, S.; Vonci, M.; Winpenny, R. E. P. *Chem. Commun.* **2002**, 1860. (b) Ferguson, A.; Parkin, A.; Sanchez-Benitez, J.; Kamenev, K.; Wernsdorfer, W.; Murrie, M. *Chem. Commun.* **2007**, 3473.